American Journal of Physical Chemistry
2023; 12(1): 7-16
http://www.sciencepublishinggroup.com/j/ajpc
doi: 10.11648/j.ajpc.20231201.12
ISSN: 2327-2430 (Print); ISSN: 2327-2449 (Online)

Photocatalytic Epoxidation of Propylene with Bi_2WO_6-Based Catalyst Supported on Glass Beads

Emmanuel Alhassan Kamba[1], Qiao Chen[2]

[1]Chemical Sciences Department, Federal University Wukari, Wukari, Nigeria

[2]Chemistry Department, School of Life Sciences, University of Sussex, Brighton, UK

Email address:

eacambah@gmail.com (Emmanuel Alhassan Kamba)

To cite this article:

Emmanuel Alhassan Kamba, Qiao Chen. Photocatalytic Epoxidation of Propylene with Bi_2WO_6-Based Catalyst Supported on Glass Beads. *American Journal of Physical Chemistry*. Vol. 12, No. 1, 2023, pp. 7-16. doi: 10.11648/j.ajpc.20231201.12

Received: September 6, 2022; **Accepted**: October 29, 2022; **Published**: March 31, 2023

Abstract: The photo activities of some photo-catalysts including TiO_2, Bi_2WO_6 and Bi_2WO_6-TiO_2 (in various mixing ratios) were evaluated for photo-epoxidation of propylene. The photocatalytic epoxidation reaction was performed in gas-phase under atmospheric pressure. Typical reaction mixture of C_3H_6:O_2:N_2 corresponding to the ratio 1:1:18, afforded PO (PO) in addition to other products such as acetone, acetaldehyde and propanal as observed by the FTIR-GCMS tandem analysis. It was established from the results that Bi_2WO_6-TiO_2 photo-catalysts were more preferable for selectivity of PO peaking at 49%. The highest formation rate of PO achieved was 111µmol g cat^{-1} h^{-1} over 12mol% Bi_2WO_6-TiO_2 ratio in a typical flow reaction for 1h at 345 K under UVA illumination. Under this condition the selectivity of products was also observed to be very stable. Further study on the effect of light intensity revealed that increasing the light intensity from 0.1 to 0.3mWcm^{-2} significantly increased the selectivity of PO by 5%. Higher intensity depreciated the PO selectivity. In order to study the effect of temperature on the photocatalytic epoxidation reaction, a systematic approach was followed. As raising the reaction temperature influences the distribution of products significantly, a temperature range of 335-355 K was used in the optimised reaction condition. At 355 K, it was observed that the formation of propanal was favoured which was attributed to its inhibition to be transformed into propionic acid. However, raising the reaction temperature was observed to affect the rate of reaction in two ways: first, the adsorption of PR on to the photo-catalyst which causes a decrease in the reaction efficiency was reduced and secondly, the desorption of products of reaction which in turn reveals more active sites, was improved.

Keywords: Propylene, Photo-Catalysis, Photo-Oxidation, Propylene Oxide, Photo-Reactor

1. Introduction

One of the green methods of producing PO is through photocatalytic epoxidation of PR using molecular oxygen [1]. The main idea of using this method is to utilise photo-energy at mild conditions while achieving high selectivity as well as yield of PO. Considering the unprecedented level of global chemical demand, especially due to continuous development of third world countries, industrial chemical processes such as epoxidation of alkenes become increasingly important [2]. Epoxides which are used as intermediates in the production of polymers and other organic compounds are synthesised annually in myriads of tonnes around the world. PO for example, is reported to have increased in consumption around the world from 3.9million tons in 1991 to 6.0million tons in 2009 [3]. The production is predicted to increase as demand also increases.

In recent times, a number of reports have been focused on the epoxidation of PR in gas-phase using molecular oxygen under high temperature and pressure conditions. Equation 1 below shows a schematic of this reaction as reported by Nguyen and co-workers [4].

However, the role of reaction temperature on the photocatalytic epoxidation of PR to PO is still not clear. But on a general note, even though the temperature has a significant impact on reactions such as gas–solid heterogeneous reactions, its sensitivity on heterogeneous photo-catalysis is very low. He et al. [5] observed that the conversion of styrene increased with temperature in the range of 343–383 K in their epoxidation of styrene experiment. They reported that the selectivity of epoxide first increased

from 71.7% at 343 K to 82.3% at 353 K, then dropped to about 61.7% at 383 K.

Using 20% Ag and 4% MoO_3/ZrO_2 at 400°C, 0.1 MPa and GHSV of 7500 h^{-1}, Li et al. [6] observed a 60.3% selectivity for PO. Similarly, Suo et al. [7] recorded 17.9% and 0.9% for PO selectivity and PR conversion respectively.

In an attempt to enhance the conversion and selectivity of PR and PO respectively, Cumaranatunge and Delgass [8] tested various Au content in Au/TS-1 catalyst at 473K in the presence of O_2 and H_2. They recorded 10% conversion and 76% selectivity for PR and PO respectively. More recently, Khatib and Oyama [9] reported 1.4% PR conversion and 99% PO selectivity in their work on Ti-containing silicate mesoporous material with gold using O_2 and H_2. In general, both the use of molecular oxygen and a mixture of hydrogen and oxygen over a thermos-catalyst have been reported to perform optimally. However, while the use of H_2O_2 to oxidise similar reactions may seem attractive, there are a number of factors to consider which include the extra energy lost during the reaction, the low hydrogen efficiency as well as safety requirements while handling the H_2O_2 production facilities [2].

In spite of the growing interest in the creation of photo-catalysts and their applications especially in the field of photocatalysis is yet to receive the necessary attention. Till date, only a few works have been reported on photo epoxidation of alkenes especially in gaseous-phase. Amadelli et al. [10] recorded 4.7% and 19.2% yield and selectivity respectively for PO in their photo-oxidation experiments to determine photo activity of more than 50 silica-supported metal oxides. Amano et al. [11] achieved 85 mol g cat^{-1} h^{-1} formation rate and 37% selectivity of PO in a continuous flow reaction using 01% V_2O_5 in SiO_2. But considering economic and environmental consequences, a number of the commonly used epoxidation methods require serious improvement. The use of cumene-hydroperoxide (developed in Japan in 2003) and hydrogen peroxide (developed in Belgium in 2008) as epoxidation procedures are still based on liquid-phase reactions involving several stages and require hydrogen [2, 4]. Although, the photo-epoxidation of PR is an environmentally friendly process as it can be carried out under mild conditions without the use of hydrogen, the production rate of PO still needs improvement. It is expected that in the future the direct epoxidation of PR into PO using light energy in the presence of photo-catalysts will not only be for laboratory research but also for chemical industry. As a result, in this study we aimed to develop a direct gas-phase photo-epoxidation of PR under mild conditions with emphasis on the selective production of PO using molecular oxygen as the only oxidant.

The main objective is to investigate the efficiency of a promising photo-catalyst in the direct gas-phase epoxidation of PR under mild conditions.

The optimal reaction conditions were also determined by comparing the selectivities and yields of PO for different catalyst modifications. Finally, a reaction mechanism for photocatalytic epoxidation of PR to PO was proposed by considering the known species present during the reaction.

2. Experimental

2.1. Preparation of Photo-Catalysts

Bi_2WO_6 was synthesised using a modified procedure reported by Murcia-López et al. [12], by dissolving 0.01 mol $Bi(NO_3)_3 \cdot 5H_2O$ in 10ml glacial acetic acid and 0.005mol $Na_2WO_4 \cdot 2H_2O$ in 90 ml deionised water. The bismuth solution was then added dropwise whilst stirring to the tungsten solution ensuring well dispersed particles. The milky suspension was stirred for further 1 hour. However, due to the hydrolysis of Bi $(NO_3)_3$, the suspension was found to be strongly acidic (pH 1.2). Therefore, an aqueous solution of sodium hydroxide (1.0mol L^{-1}) was added to adjust the pH of the suspension. The suspension was then hydrothermally treated at 140°C for 16 hours using autoclaves. The suspension was filtered and rinsed with deionised water and dried in an oven at 80°C overnight. The dried powder was then ground and calcined at 300°C for 4 hours.

Bi_2WO_6/TiO_2 was prepared using the same synthesis procedure as above for the preparation of the Bi_2WO_6 precursor. TiO_2 precursor was prepared as follows: 0.1mL of distilled water and 10mL of isopropanol were mixed separately then added dropwise to a mixture containing 2.5g of titanium (IV) isopropoxide (TTiP) as the Ti source and 10 mL of isopropanol. The solution was stirred in an oil bath at 80°C for 18 hr. An amount of 6 mL of acetyl acetone was then added to the TiO_2 sol. Finally, the concentration of the TiO_2 sol was adjusted to 3.0wt.% by isopropanol. The final TiO_2 solution was incorporated into the milky suspension of Bi_2WO_6 before hydrothermal treatment for 16 hr. The suspension was filtered and rinsed with deionised water and dried in an oven at 80°C for 4 hours. The baked powder was then calcined at 300°C for 4 hours. The procedure was repeated with different weight ratios of Bi_2WO_6 to make 10, 30, 50 and 70wt.%. Based on the concentration of Bi_2WO_6, the obtained Bi_2WO_6/TiO_2 powders were labelled B-10/TiO_2, B-30/TiO_2, B-50/TiO_2 and B-70/TiO_2, respectively.

2.2. Characterization Techniques

The morphological analysis of the synthesised nanostructure during this study was carried out using Scanning Electron Microscope. Elemental analysis was performed on the studied samples using Energy Dispersive X-ray Spectroscopy (EDX). The band gap of the nanostructure was determined using an integrating sphere equipped with an inbuilt tungsten-halogen illumination source (300 nm± 1000 nm). The Tauc relation was applied in the determination of the band gap of the studied materials from their UV-Vis diffuse reflectance spectra. Powder X-Ray Diffraction was used for crystalline structure determination. The X-ray source was copper plate and the peak incident wavelength was at 1.54 Å. Brunauer-Emmett-Teller (BET) specific surface area was measured using nitrogen adsorption at 77 K on a surface area and pore size analyser.

2.3. Photocatalytic Epoxidation of PR

All photocatalytic epoxidation experiments were conducted in a flow reaction set up. Typical reaction gas mixture was C_3H_6:O_2:N_2 = 1:1:18 at a gas hourly space velocity (GHSV) of approximately 6000 h^{-1} under ambient conditions. 5mgg^{-1} of the photo-catalyst was immobilised on glass beads using an improved spray coating technique developed in this work. The packed catalyst coated beads were brought in contact with the reacting gaseous mixture through the reactor inlet under the illumination of UVA (Figure 1).

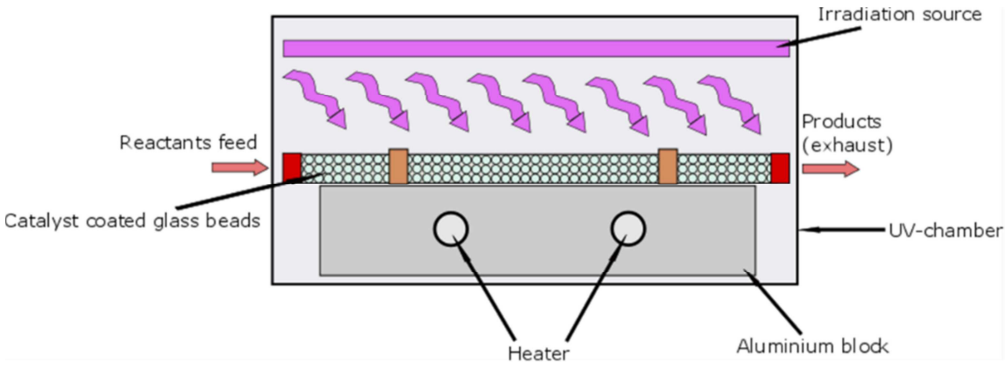

Figure 1. *Scheme of reactor.*

A flow of propylene, oxygen and nitrogen was mixed together in a mixing chamber and fed directly to the reactor through the inlet to establish contact with the catalyst. The photo-reactor was also placed on an aluminium block modified with heating cartridges in order to measure the effect of temperature on the reaction system. The heating system was controlled with regulator to give accurate reading. The maximum temperature of the dead reactor was determined to be 335 K and thus, was regarded as the initial reaction temperature. Photoreaction study was carried out at elevated temperatures of 345 and 355 K. A Cross linker equipped with 5 x 200W mercury–arc lamps was used to source for UV-A light (wavelength 320–500 nm). Since the light intensity of the UV chamber was fixed (not adjustable), it was considered the minimum light intensity for the entire study. A Compact illuminator 6000CI Xenon Light Source was also used to further increase the light intensity in order to study its effect on the photoreaction process. Finally, the effect of O_2 concentration on the reaction was investigated by altering the O_2/N_2 ratio.

The exhaust from the reactor was analysed directly using a purpose built Fourier Transform Infrared Spectroscopy (FTIR) flow cell with NaCl windows and a Gas Chromatograph Mass Spectrometry (GCMS) auto-sampling system developed in this work (Figure 2); which were controlled by automated system softwares (auto-clicker) for the FTIR and auto-sampler for the GCMS using MS Workstation software. The outlet of the flow cell was directly connected to a GCMS auto-sampling vial (modified for the purpose) in a tandem FTIR-GCMS analysis. In this way, data was collected from both instruments simultaneously. PerkinElmer Spectrum One FTIR was used to analyse the concentration of reactants and products. Varian CP-3800 gas chromatograph was used to separate the compounds and a Varian Saturn 2000 mass spectrometer was used to analyse the separated products. For separation of epoxidation products of propylene, a PLOT column, Rt-QS-BOND 30m x 0.53mmID x 20um was used. The MS/detector end of this column was coupled with 25cm of a 0.25mmID x 0.25umdf column using a RESTEK siltite micro union to trap the particles coated within the PLOT column and prevent contaminating the MS trap assembly. A carrier gas of helium was used at a flow rate of 100ml min^{-1}. The MS was performed through electron ionisation (EI).

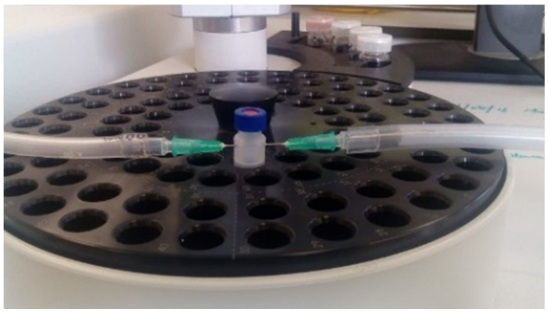

Figure 2. *Auto-sampling vial modification.*

Prior to photoreaction, the adsorption of PR on the catalyst surface is determined by integrating the concentration profiles of the dark equilibrium adsorption data of propylene. The UV lights were then switched on to initiate photoreaction. This process was repeated for all the studied catalysts.

The following equations were used to calculate PR conversion, consumption and adsorption rates, and the selectivity of products for the reaction.

$$C_3H_6\ consumption\ rate\ = C_3H_6\ feed\ rate - \ C_3H_6\ out\ rate \quad (1)$$

$$C_3H_6\ conversion\ rate\ = rate\ of\ all\ products\ covered\ to\ C3\ products \quad (2)$$

$$C_3H_6\ adsorption\ rate = C_3H_6\ consumption\ rate\ - \ C_3H_6\ conversion\ rate \quad (3)$$

$$Product\ selectivity = \frac{moles\ of\ the\ formation\ one\ C3\ product}{moles\ of\ all\ C3\ products} x100\% \quad (4)$$

3. Results and Discussions

3.1. Photo-Catalyst Characterization

The X-ray diffraction patterns, depicting the crystal structure of the synthesised photo-catalysts are shown in Figure 3. Bi_2WO_6 peaks indicate that it was formed in the russellite phase as suggested by the database (JCPDS 39-0256). However, all samples of Bi_2WO_6/TiO_2 as well as pure TiO_2 exhibited peaks associated with both compounds. The (101) surface of anatase phase of TiO_2 (JCPDS 21-1272) appeared in all the peaks of the samples indicating that TiO_2 was well incorporated into the Bi_2WO_6. The broadness of the diffraction peaks of Bi_2WO_6 indicates the low levels of crystal structures which has been reported to be due to the unordered nature of the sample causing the diffraction to stretch over several 2θ values. The crystal sizes of the prepared Bi_2WO_6 were determined using the Scherer's equation. The FWHM of the peak with the highest intensity; (131) corresponding to diffraction peak 28.8° was considered. The mixture of Bi_2WO_6 and TiO_2 also showed comparatively broader peaks indicating that the mixture had little or no effect on the crystal structure of the Bi_2WO_6.

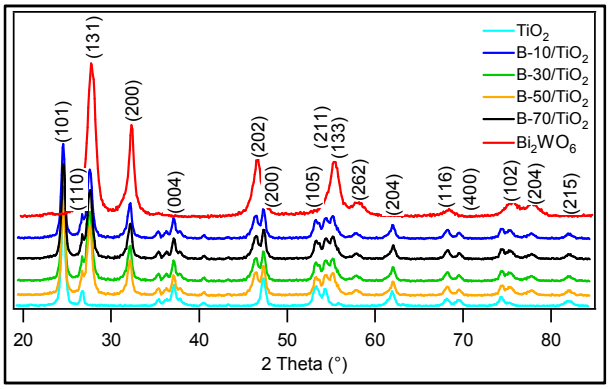

Figure 3. *XRD spectra of Bi_2WO_6, mixtures of the 2 compounds and TiO_2.*

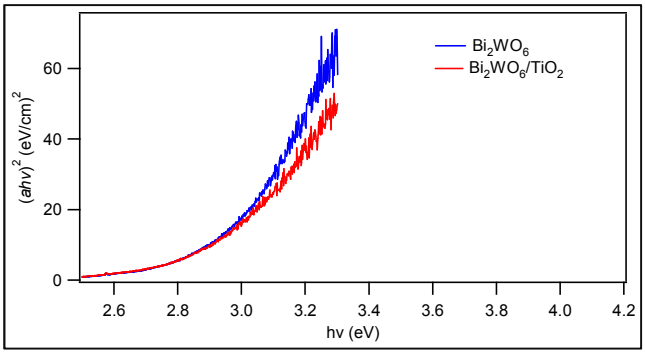

Figure 4. *Tauc plot of the reflectance spectra of Bi_2WO_6 and Bi_2WO_6/TiO_2. The linear portion shown in red segmented lines indicate the extrapolation of the nanostructures' band gaps.*

Tauc plot generated from the UV-Vis reflectance spectra of the synthesised photo-catalysts is shown in Figure 4. The linear nature of the Tauc plot, suggested that the materials are semi conductive in nature. Moreover, it was possible to determine from the plot that the synthesised pure Bi_2WO_6 has a band gap of 2.89 ± 0.05eV while the addition of TiO_2 to the Bi_2WO_6 gave resulted in a blue shift with a band gap of 2.75 ± 0.06eV. The experimentally determined band gap of Bi_2WO_6 powder is in agreement with the literature.

Due to its lower band gap (2.89eV), the synthesised Bi_2WO_6 nano-flowers can be considered a suitable alternative to larger band gap (3.06 eV) of pure TiO_2 nanoparticles. The Bi_2WO_6 nano-flowers will therefore be expected to be more energetically efficient in the photo-epoxidation process. It is also important to note that combination of both catalysts reduces the rate of recombination of the charged particles.

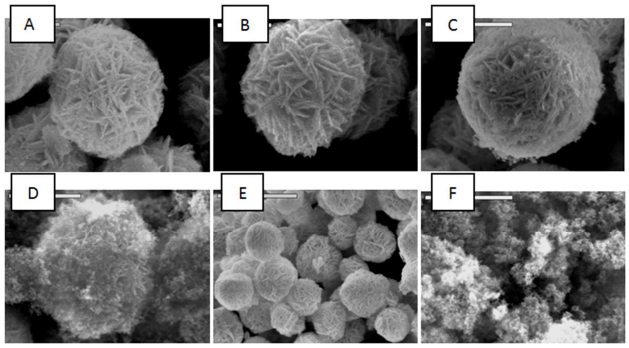

Figure 5. *SEM images of hydrothermally synthesised Bi_2WO_6 Nano flowers: (A) Bi_2WO_6 (B) B-1/TiO_2 (C) B-3/TiO_2 (D) B-5/TiO_2 (E) Uniform distribution of nano flower balls (F) TiO_2.*

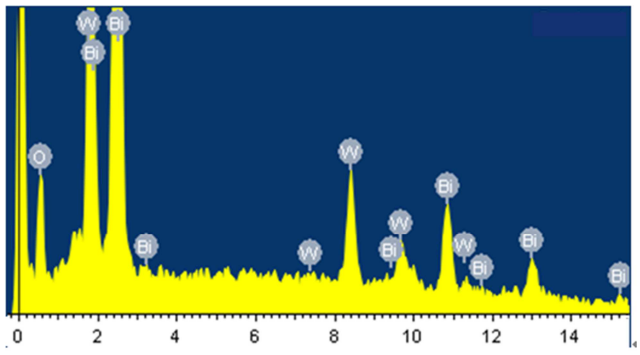

Figure 6. *EDX of (a) Bi_2WO_6 and (b) Bi_2WO_6/TiO_2.*

The SEM images of hydrothermally synthesised Bi_2WO_6 and Bi_2WO_6/TiO_2 are shown in Figure 5. The formation of spherical structures with clearly define stack of aggregate sheets otherwise known in the literature as "nano flowers" or "nano flakes" can be seen. Figure 5A and B show typical bismuth tungstate particle of average size of 2 nm formed through the Ostwald-ripening process. These nano sheets are centred on a nucleation site to produce this flower like structures, the size of which depends on the mixing ratio of the reacting species and are well documented in literature. This morphology gives the catalyst a high surface area to volume ratio which is beneficial for adsorption of substrates. Figure 5C, D and E show the images of TiO_2

incorporated Bi_2WO_6 of 10, 30, 50 and 70 wt%. It can be seen that increasing the concentration of the latter material caused a readily observable change in the morphology of the particles. There was a progressive decrease in the 3D-hierarchical architecture until a structure similar to that of TiO_2 (Figure 5F) was obtained. This indicates that presence of TiO_2 can inhibit the growth process of the nucleation sheets resulting in decreased particle size of pure Bi_2WO_6. On the other hand this, the reduction in particle size due to increased amount of TiO_2 could be beneficial to the coating of the catalyst on the glass beads resulting in an increased surface area of the mixed catalyst.

Figure 6 shows the EDX data at 1 keV of the synthesised materials. It can be seen that a relatively pure material was obtained.

3.2. Glass Bead Supported Photo Catalyst Efficiency

Glass beads coated with synthesised catalysts through the spray technique were studied as an alternative to the conventional catalyst immobilisation such as dip coating on glass rods, activated carbon etc. A test on the stability of the catalyst coating carried out by immersing the catalyst coated beads in both aqueous and non-aqueous liquids revealed promising results. Indeed, only a minimal loss of catalyst (an average loss of 2 ± 0.5 mg of the catalyst was observed from samples containing 28.6 mg of the catalyst). This improved adhesion of the catalyst on the glass beads can be attributed to the base pre-treatment of the glass beads which formed OH functional groups on the glass surface, thus allowing the generation of a chemical bond between the catalyst and the glass, effectively ensuring an enhanced adhesion of the system. Furthermore, it can be seen from the 2D flow dynamics simulation in Figure 7 that the velocity of the fluid flowing through the photocatalytic reactor made with spherical glass supports display major improvements as spherical systems do not induce laminar but rather turbulent flows when coming in contact with fluid streams.

It can also be seen from Figure 7 that the lack of preferential flow channels is readily apparent as the fluid maintains a homogeneous velocity throughout the whole system. It is of further importance to note that the fluid velocity at the surface of the beads is close to that in the bulk fluid, meaning that a greater gas/catalyst contact can be achieved. The observation of turbulent, rather than laminar, fluid flows over glass spheres is consistent with the calculations and observations of [13] during their study of fluid flows in randomly packed porous bed reactors.

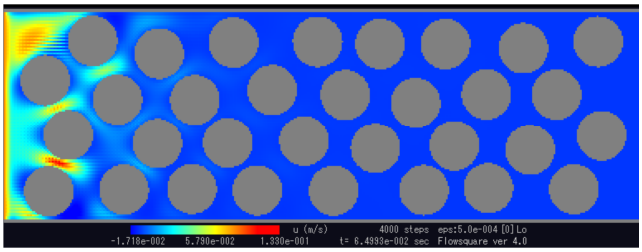

Figure 7. *Results of the flow dynamic simulations carried out showing the velocity of the gas flow in 2D cross-sections of the photoreactor over glass beads supported catalysts. 2D flow dynamic simulations were carried out using the Flowsquare flow dynamic simulation software taking into account the experimental gas flow rate, density and temperatures.*

3.3. Direct Gas-Phase Photocatalytic Epoxidation of PR

During the epoxidation experiments, no activity was observed in the absence of either photo-catalyst or UV illumination suggesting that the epoxidation reactions over the studied photo-catalysts were mainly photocatalytic. The results of photo-epoxidation of PR with molecular oxygen over the studied photo-catalysts in a flow reactor at mild conditions are summarized on Table 1. Our homemade TiO_2 on Table 1 (entry 1) showed high photo-oxidation activity with PR consumption rate of 619.5 mol g^{-1} h^{-1}. CO_2 was the major product while no PO was observed. Excess production of CO_2 can be attributed to the successive photo-oxidation of oxygenated by-products. Entry 2 of Table 1 shows that under the given conditions, only a low amount of PO was produced at a formation rate of 0.31 µmol $g^{-1}h^{-1}$ when only Bi_2WO_6 was used in photo-catalytic epoxidation reaction. Entries 3-6 show as expected that the highest photo-catalytic performance was obtained with Bi_2WO_6/TiO_2. B-30/TiO_2 achieved the highest PO formation rate (entry 4) which diminished with increase in the Bi_2WO_6 coupling amount to achieve PO formation rates of 4.7 and 3.9 µmol $g^{-1}h^{-1}$ for B-50/TiO_2 and B-70/TiO_2 respectively (entries 5 & 6). These observations can be attributed to the presence of sufficient amount of electron trap while still not blocking the active sites on the TiO_2 lattice. All combinations of photo-catalysts were active and stable for the production of PO, irrespective of the differences in their optimal conditions.

Table 1. *Photocatalytic epoxidation of PR.*

Entry	Catalyst	BET surface area (m^2g^{-1})	Temp (K)	PR		PO formation rate (µmol $g^{-1}h^{-1}$)
				Adsorption rate (µmol $g^{-1}h^{-1}$)	Conversion rate (µmol$g^{-1}h^{-1}$)	
1	TiO_2	50.0	335	0.04	619.5	-
2	Bi_2WO_6	37.8	335	0.06	455.4	0.31
3	B-10/TiO_2	67.2	335	0.07	723.5	2.4
			335	0.08	882.5	5.2
4	B-30/TiO_2	69.7	345	0.06	902.4	3.6
			355	0.05	891.3	6.2
5	B-50/TiO_2	53.5	335	0.06	882.5	5.2
6	B-70/TiO_2	46.9	335	0.06	882.5	5.2

Reaction conditions: photo-catalyst 0.02 g; feed gas C_3H_6:O_2:N_2 = 1:1:18 vol% at a gas hourly space velocity (GHSV) of 6000 h^{-1}. The data is the mean value obtained on stream after 1 h.

A negative trend was observed in PR adsorption with increase in temperature over B-30/TiO_2 catalyst. This catalyst also presented the highest surface area according to our BET data, which could be the likely reason for the highest adsorption of PR at 335 K. All the photo-catalysts displayed adsorption of PR during photoreactions upon light illumination. This was observed in the sudden rise in concentration of the reactant immediately lights were turned on. This indicates that the adsorbed organics were being desorbed from the surface of catalysts upon initialising the reaction. The average adsorption rates based on the carbon balance within the reaction period are shown on Table 1. PR adsorption was considered the combination of physical and chemical adsorptions on the photo-catalysts, which largely depends on surface area as well as TiO_2 content. It is believed that due to the presence of nucleation sheets on the surface of the Bi_2WO_6 catalyst a substantial amount of PR was adsorbed. Therefore, presence of Bi_2WO_6 enhanced harvesting of more photo-energy to produce sufficient amount of charged particle pairs that carried out the partial oxidation of PR [14].

Figure 8 shows the results of the photo-epoxidation of PR over the catalysts. It can be seen the CO_2 dominated the products of epoxidation over TiO_2 (Figure 8A). This was expected as TiO_2 is known for its ability to completely mineralise alkenes to CO_2 as was also observed in this work. However, coupling Bi_2WO_6 with TiO_2 resulted in the formation of PO achieving the highest selectivity of 65% with B-30/TiO_2. When the concentration of Bi_2WO_6 was increased in the catalyst mixture to 50 and 70%, a continuous decrease in PO selectivity was observed (Figure 8B). Bi_2WO_6 efficiency as a photo-catalyst lies within the hybridisation that exist between O 2p and Bi 6s orbitals in the valence band. Two effects may be responsible for the photocatalytic properties: first, under visible irradiation there will be an electronic transition to the W 5d orbitals in the conduction band. Secondly, the mobility of hole can be greatly favoured due to large dispersion in the valence band [15-17]. To compare the selectivities of all the products of photo-epoxidation of propylene, Figure 8C was plotted as obtained using the best catalyst in this work; B-30/TiO_2 after 10 min of UV illumination. It can be seen that PO remained the dominant product with selectivity of 64.7% followed by CO_2 21.3%.

Other products observed during the photo-epoxidation of PR with molecular oxygen and their selectivities are: acetone (12.6%) and acetaldehyde (1.4%). The results obtained in this work show that mixing appropriate amount of Bi_2WO_6 and TiO_2 has potential of an ideal catalyst for partial oxidation of organic compounds. Considering that our homemade TiO_2 formed no PO as also reported of P25 in literature, it demonstrates the key role played by Bi_2WO_6 in the selectivity of PO. Therefore, it is necessary to further evaluate the activity of the combined catalyst. Although the exact role of Bi_2WO_6 in the coupled photo-catalyst used in epoxidation reactions is still a subject of debate, it is expected to contribute in enhancing the charge separation mechanism thus, increasing the selectivity of epoxides.

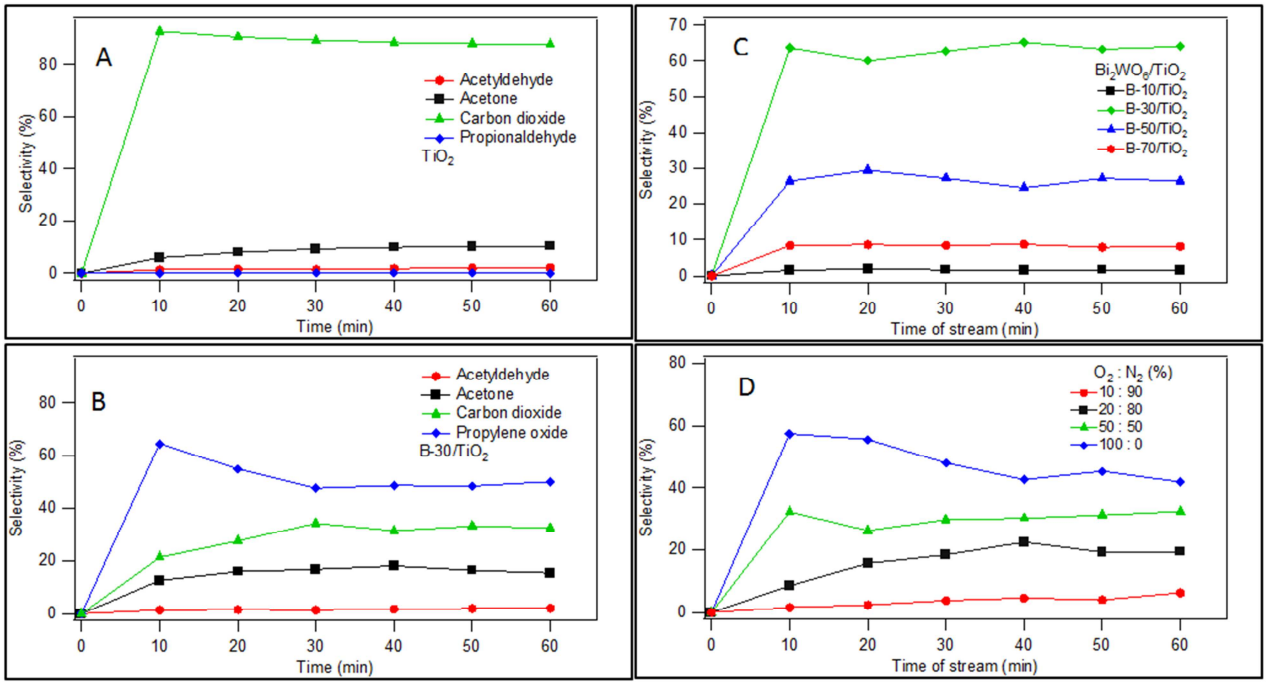

Figure 8. *The time-dependent behaviour of selectivity for the formation of PO, AC, CO_2 and H-CHO over different catalyst mixture at different conditions: (A) TiO_2; (B) Bi_2WO_6/TiO_2; (C) B-30/TiO_2 and (D) O_2: N_2 ratios.*

Moreover, increasing the Bi_2WO_6 concentration to 30% from 10% presented an improvement in the selectivity of PO which perhaps could be due to the majoritarian presence of Bi_2WO_6; but also oxidation of PR by TiO_2. This result agrees

with the findings of [10] in their photocataytic epoxidation of PR study. They observed coupling Bi_2WO_6 and TiO_2-P25 in a 1-1 ratio resulted in improved PR conversion (10%) and PO selectivity (50%) compared to same coupled photo-catalyst with lower amount of Bi_2WO_6.

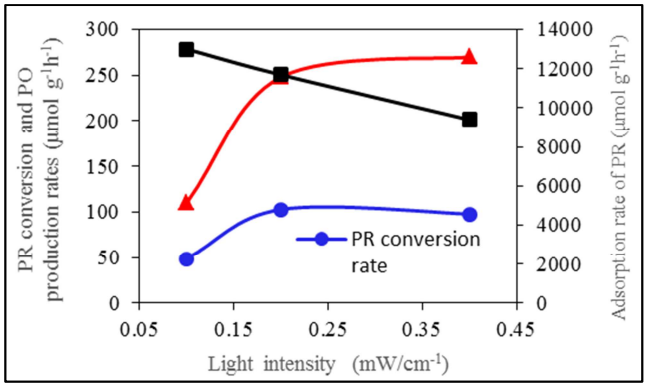

Figure 9. *The light effect on PR conversion and adsorption rates and PO formation, with Bi_2WO_6/TiO_2.*

3.4. Effect of Temperature on Photo-Epoxidation

Although PO was still the dominant product at the optimum reaction conditions of this work, there was a slight increase in concentration of acetone and alcohol at 70°C. Further increase in temperature to 80°C showed a substantial amount of increase in propanal concentration while that of PO remained constant. This suggests that temperature can affect the adsorption and desorption of the PR and reaction products respectively on the photo-catalyst. Increasing the temperature would inhibit the adsorption process, since adsorption itself is an exothermic process. Nevertheless, high temperature favours desorption process as it is an endothermic process. Figure 10 shows the result of experiments performed to elucidate the temperature effect on the photo-epoxidation reaction. It can be seen that no monotonic correlation exists between the rate of epoxidation and reaction temperature.

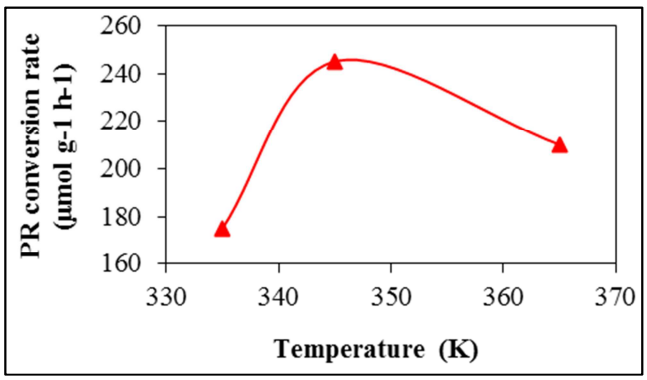

Figure 10. *The effect of reaction temperature on photocatalytic epoxidation rate. The PR conversion rate was obtained on stream after 4h.*

Photo-reactions are generally known to proceed without requiring any form of heat due to photonic excitation. However, increasing the temperature enhances efficiency of the photo-catalytic reaction by increasing desorption of reaction products which in turn releases more active sites for more reactions. Kim and Lee [18] explained in their study on the Effect of pH and temperature on photocatalytic degradation of organic compound on carbon-coated TiO_2, that since there is no true activation energy, *Et,* in photo-reaction, the activation energy would be the very small apparent activation energy, *Ea*. Consequently, the desorption rate of final product is considered the limiting step while apparent activation energy tends toward the heat generated as the products are adsorbed within the medium temperature range. The results in Figure 11 show that the reaction efficiency increased within the range of 335–345 K while further increase in the temperature to 365 K only resulted in difficulty in adsorption of PR on the photo-catalyst. Consequently, the reaction efficiency was observed to reduce (Figure 11). This is consistent with the results obtained by Nguyen et al. [4].

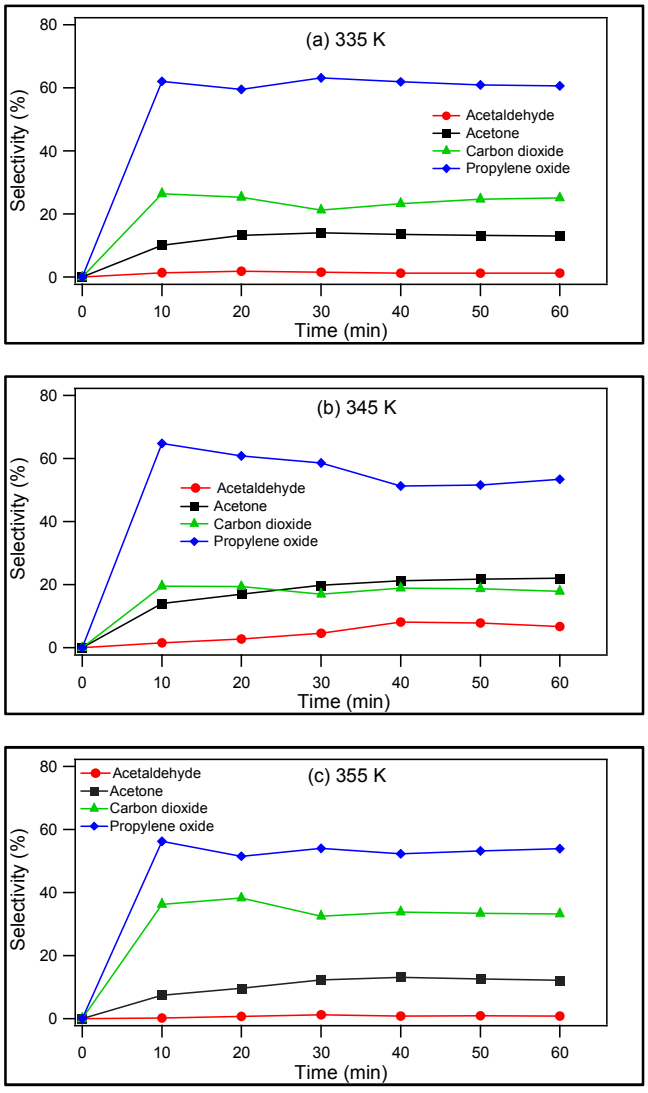

Figure 11. *The selectivity of epoxide products on stream for different temperature conditions: (a) 335 K; (b) 345 K and (c) 355 K.*

Figure 12. *Colour change observed before (left) and after (right) the illumination.*

The high stability in the selectivity of products on stream as well as similarity in time-dependent behaviour of the photocatalytic epoxidation reaction. The selectivities of products gradually increased with rise in temperature. However, when the temperature rose above 345 K, a slight decrease in selectivity of PO was observed. This decrease is attributed to increased competition of multiple reactions towards different products as is widely known that upon irradiation of a photo-catalyst with UV, several reactions occur leading to generation of active species.

3.5. Photochromism of Bi_2WO_6

Upon irradiation of the coated coupled Bi_2WO_6/TiO_2 photocatalyst sample with UV light a dramatic change of colour from bright yellow to black was observed (Figure 12A). This change in colour only occurred with Bi_2WO_6 alone or when coupled with TiO_2. No colour change was observed with TiO_2 alone (Figure 12B left) after illumination (Figure 12B right). Although the colour change was only slightly grey after 15 min of illumination, the colour change progressively became saturated as the reaction continued.

Figure 13. *Effect of coating time of the catalyst on colour change after an hour of irradiation.*

Another observation made was the amount of time required to coat the catalyst on to the beads which seems to have an impact on the homogeneity of the colour change. After 30 min of ball milling 5 milligram of the catalyst per gram of the beads, a rather dull unsmoothed coated beads were obtained. But when the coating time was increased to an hour, a shinier finished product was obtained (Figure 12B). Subjecting both coated samples to UV illumination gave two different results. While 30 min of coating didn't give complete change of colour as traces of grey coloured beads were observed after an hour of irradiation, 60 min of coating gave more or less a completely black product (Figure 13). This observation could be attributed to the electromagnetic field generated during the milling process. As the beads continued to rub against the wall of the container in the presence of the catalyst, they become more magnetic. The more the milling time, the higher the magnetic effect. Figure 13 shows the magnetic hysteresis loops of Bi_2WO_6 coated glass beads coated for 30 and 60 min. It can be seen that the magnetisation saturation of the 60 min coating is twice that 30 min by a factor of 2. This also shows that the magnetic field of the former is higher.

4. Proposed Mechanism of Photocatalytic Epoxidation

Although the intrinsic photo-epoxidation mechanism is still a subject of debate, herein a possible route for the reaction is proposed bearing in mind the reacting species present during the photo-epoxidation reaction. At steady state, light was irradiated and an electron/hole (e^-/ h^+) pair was generated in the photo-catalyst as in equation (5).

$$\text{Photocatalyst} \xrightarrow{h\nu} e^- + h^+ \tag{5}$$

$$O_{2(g)} \rightarrow e^- + O^-_{2(ads)} \tag{6}$$

$$O^-_{2(ads)} + h^+ \rightarrow 2O^*_{(ads)} \tag{7}$$

Adsorbed O_2 is reduced to superoxide, O_2^- when reacted with an electron as shown in equation (6). Due to the stable nature of $O_2^-{}_{(ads)}$ species, it is not directly involved in the process. Atomic oxyradicals which are formed during the reaction between the preceding species and the positively charge hole are the active species as seen in equation (7) below.

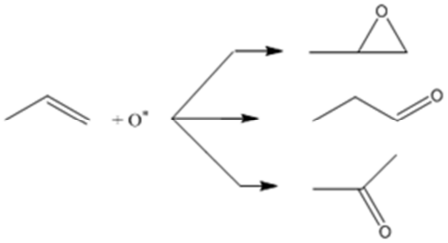

(8)

Approximately 80 to 90% of the reaction products are known to be formed when the surface atomic oxyradicals as

in equation (8) above react with PR in the epoxidation reaction. Equation (8) shows some of the several pathways to create the products. Figure 14 shows the schematic for the selective oxidation of PR to PO as proposed by Carter and Goddard [19], they suggested that the reaction occurs via H-atom abstraction resulting in the formation of oxypropenyl intermediate. The selectivities of products depend on both the angle at which the H-atom is abstracted from the PR when attacked by $O_{(ads)}*$ and the conditions of reaction.

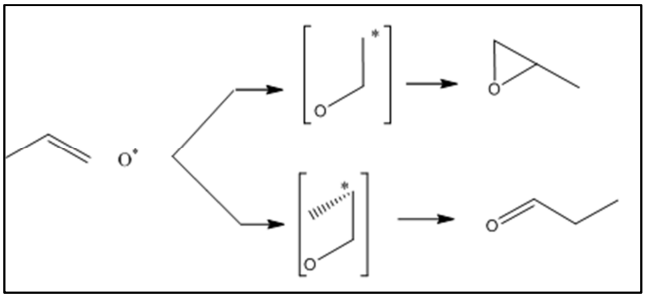

Figure 14. *Scheme: The formation mechanism of PO and oxygenate products over Bi_2WO_6/TiO_2 photo-catalyst.*

Due to size of the nucleation sheets in the photo-catalyst, the formation of intermediate species of PO as well as another product via H-atom abstraction will occur in a limited space. For instance, while oxypropenyl intermediate of PO is formed within an available space, due to space limitation the intermediate of propanal could be inhibited from forming. Therefore, it could be suggested that the selectivity of PO could be enhanced due to space restriction in the Bi_2WO_6/TiO_2 catalyst.

5. Conclusions

One of the emerging energy conservation technologies today is the use of light energy to produce PO from PR in the presence of a photo-catalyst. As the choice or production of a suitable catalyst remains a challenge, several photo-catalysts have been tested for this purpose. Herein, we presented a direct photo epoxidation process to produce PO from PR by O_2 with the aid of light energy over photo-catalysts under mild conditions. In contrast to the conventional thermal processes of PR epoxidation, no hydrogen was needed in the photocatalytic process. This study shows that even though TiO_2 has high photocatalytic activity, it is not ideal for partial oxidation of PR to PO under the studied reaction conditions. Instead, it completely mineralises the reactant into CO_2 and H_2O as the main reaction products. The concentration of Bi source in the created catalyst has shown to affect the efficiency of photo epoxidation process. With moderate amount of Bi_2WO_6 to TiO_2 ratio, it was possible to achieve the highest PO formation rate and selectivity of 114 mol g cat^{-1} h^{-1} and 47%, respectively, at 345 K and atmospheric pressure with minimal production of CO_2. It could therefore be said that in this study, the photocatalytic epoxidation of PR in the presence of molecular oxygen in a flow reaction setup, was enhanced with Bi_2WO_6/TiO_2. PO production could also be possibly enhanced further by overcoming the space limitation posed by the nucleation sheets of the photo-catalyst thereby unrestricting the reaction of intermediates. Additional light source was used to increase light intensity in this work. It was possible to evaluate the effects of light intensity on the epoxidation reaction and achieve an optimum work intensity of $0.2mW/cm^2$. The photo catalytic epoxidation of PR can be performed at room temperature as the reaction can be initiated by photons. However, when the effect of temperature on the photocatalytic epoxidation of PR over the studied photo catalyst was investigated, it was revealed that there exists an optimum temperature that favours the production of PO, 345 K. The results obtained in this work also show that the effect of temperature on the photo-epoxidation reaction temperature is two-fold. While increase in temperature accelerates surface reaction, it can also lead to decrease in the adsorption of reactants on the surface of the photo-catalyst. At higher temperature, the partial oxidation becomes impeded resulting in re-arrangement in the distribution of products formation with propanal being more favoured.

References

[1] E. Klemm et al., "Direct gas-phase epoxidation of propene with hydrogen peroxide on TS-1 zeolite in a microstructured reactor," Ind. Eng. Chem. Res., vol. 47, no. 6, pp. 2086–2090, 2008.

[2] P. Ferrandez, "Alternatives for the production of propene oxide," 2015.

[3] X. Lang, X. Chen, and J. Zhao, "Heterogeneous visible light photocatalysis for selective organic transformations," Chem. Soc. Rev., vol. 43, no. 1, pp. 473–486, 2014.

[4] V.-H. Nguyen, H.-Y. Chan, J. C. S. Wu, and H. Bai, "Direct gas-phase photocatalytic epoxidation of propylene with molecular oxygen by photocatalysts," Chem. Eng. J., vol. 179, pp. 285–294, 2011.

[5] J. He, Q. Zhai, Q. Zhang, W. Deng, and Y. Wang, "Active site and reaction mechanism for the epoxidation of propylene by oxygen over $CuOx/SiO_2$ catalysts with and without Cs+ modification," J. Catal., vol. 299, pp. 53–66, Mar. 2013.

[6] N. Li, B. Yang, M. Liu, Y. Chen, and J. Zhou, "Synergetic photo-epoxidation of propylene with molecular oxygen over bimetallic Au–Ag/TS-1 photocatalysts," Chinese J. Catal., vol. 38, no. 5, pp. 831–843, May 2017.

[7] Z. Suo, M. Jin, J. Lu, Z. Wei, and C. Li, "Direct gas-phase epoxidation of propylene to propylene oxide using air as oxidant on supported gold catalyst," J. Nat. Gas Chem., vol. 17, no. 2, pp. 184–190, Jun. 2008.

[8] L. Cumaranatunge and W. N. Delgass, "Enhancement of Au capture efficiency and activity of Au/TS-1 catalysts for propylene epoxidation," J. Catal., vol. 232, no. 1, pp. 38–42, 2005.

[9] S. J. Khatib and S. T. Oyama, "Direct Oxidation of Propylene to Propylene Oxide with Molecular Oxygen: A Review," Catal. Rev., vol. 57, no. 3, pp. 306–344, Jul. 2015.

[10] R. Amadelli, L. Samiolo, A. Maldotti, A. Molinari, and D. Gazzoli, "Selective photooxidation and photoreduction processes at Tio 2 surface-modified by grafted vanadyl," Int. J. Photoenergy, vol. 2011, 2011.

[11] F. Amano, K. Nogami, R. Abe, and B. Ohtani, "Preparation and Characterization of Bismuth Tungstate Polycrystalline Flake-Ball Particles for Photocatalytic Reactions," J. Phys. Chem. C, vol. 112, no. 25, pp. 9320–9326, Jun. 2008.

[12] S. Murcia-López, V. Vaiano, D. Sannino, M. C. Hidalgo, and J. A. Navío, "Photocatalytic propylene epoxidation on Bi_2WO_6-based photocatalysts," Res. Chem. Intermed., vol. 41, no. 7, pp. 4199–4212, Jul. 2015.

[13] V. A. Patil, J. A. Liburdy, and J. Homepage, "Turbulent flow characteristics in a randomly packed porous bed based on particle image velocimetry measurements Additional information on Phys. Fluids Turbulent flow characteristics in a randomly packed porous bed based on particle image velocimetry measurements," Cit. Phys. Fluids, vol. 25, p. 43304, 2013.

[14] A. V. Vorontsov, D. V. Kozlov, P. G. Smirniotis, and V. N. Parmon, "TiO_2 photocatalytic oxidation: II. Gas-phase processes," Kinet. Catal., vol. 46, no. 3, pp. 422–436, 2005.

[15] M. M. Khan, S. F. Adil, and A. Al-Mayouf, "Metal oxides as photocatalysts," Journal of Saudi Chemical Society, vol. 19, no. 5, pp. 462–464, 2015.

[16] M. Qiu et al., "Synthesis of Ti 3+ self-doped TiO 2 nanocrystals based on Le Chatelier's principle and their application in solar light photocatalysis."

[17] S. M. Gupta and M. Tripathi, "A review of TiO_2 nanoparticles," Chinese Sci. Bull., vol. 56, no. 16, pp. 1639–1657, 2011.

[18] J. S. Kim and T. K. Lee, "Effect of humidity on the photocatalytic degradation of trichloroethylene in gas Phase over TiO_2 thin films treated by different conditions," Korean J. Chem. Eng., vol. 18, no. 6, pp. 935–940, Nov. 2001.

[19] E. A. Carter and W. A. Goddard, "Chemisorption of oxygen, chlorine, hydrogen, hydroxide, and ethylene on silver clusters: A model for the olefin epoxidation reaction," Surf. Sci., vol. 209, no. 1–2, pp. 243–289, Feb. 1989.